

as a product. Both acidic and neutral pH conditions give essentially the same oxidation rates and the same products. To inhibit product racemization and to increase solubilities, we carried out oxidations where CD spectra were obtained near neutral pH. In basic solution, the tartrate complexes are destroyed by permanganate, giving chromate as one product.

The CD spectra (corrected for presence of unreacted optically active starting material) of the products of the oxidations of $[\text{HCr}_2(d\text{-tart})_2(\text{bpy})_2]^-$ and $(\text{CD}^+)_{589}\text{-}[\text{HCr}_2(ms\text{-tart})_2(\text{bpy})_2]^-$ have maxima and relative band intensities in agreement with those reported for $[\text{Cr}(\text{ox})_2(\text{bpy})]^-$.⁶ The linear log plots obtained from the time dependence of these spectra show that the products of the *d*-tartrate and *ms*-tartrate complex oxidations racemize in first-order reactions with $t_{1/2}$ values of 48 and 46 min, respectively, at 23 °C. These values are reasonably close to that of 63 min at 25 °C calculated for the same conditions of pH and ionic strength from kinetic parameters for racemization of $[\text{Cr}(\text{ox})_2(\text{bpy})]^-$;⁷ however, the values measured for our products are undoubtedly lowered, owing to catalysis by the Mn^{2+} ions present.⁷ Comparisons of CD spectra for reactions and products in these oxidations permit chemical correlations of the absolute configuration of $[\text{HCr}(d\text{-tart})_2(\text{bpy})_2]^-$ (which must be Δ at chromium)³ with that of $(\text{CD}^-)_{513}\text{-}[\text{Cr}(\text{ox})_2(\text{bpy})]^-$ and of the absolute configuration of $(\text{CD}^+)_{589}\text{-}[\text{HCr}_2(ms\text{-tart})_2(\text{bpy})_2]^-$ with that of $(\text{CD}^+)_{513}\text{-}[\text{Cr}(\text{ox})_2(\text{bpy})]^-$. These correlations are based on the not unreasonable assumption that oxidation occurs with (at least, primarily) retention of configuration at chromium, and they are in agreement with previous assignments³ of opposite absolute configurations to $[\text{HCr}_2(d\text{-tart})_2(\text{bpy})_2]^-$ and $(\text{CD}^+)_{589}\text{-}[\text{HCr}_2(ms\text{-tart})_2(\text{bpy})_2]^-$ on the basis of CD spectra alone.

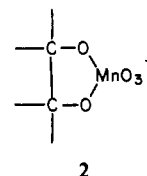
The optically active product formed in the permanganate oxidation of $[\text{HCr}_2(d\text{-tart})_2(\text{phen})_2]^-$ exhibits a CD spectrum with a major negative band at 537 nm (differing from the value of 526 nm reported for $[\text{Cr}(\text{ox})_2(\text{phen})]^-$).⁶ All of our results indicate that this product is primarily $[\text{Cr}(\text{ox})(\text{H}_2\text{O})_2(\text{phen})]^+$, which must have a *cis* configuration in order for optical activity to occur. The time-dependent CD spectra show that this product loses optical activity in a first-order reaction at $T = 23$ °C, $\mu = 1.00$ M, and pH 6.1 with $t_{1/2} = 41$ min (in the presence of Mn^{2+}). This oxidation reaction shows that the chromium absolute configurations of $[\text{HCr}_2(d\text{-tart})_2(\text{phen})_2]^-$ (which is Δ)³ and $(\text{CD}^-)_{537}\text{-}[\text{Cr}(\text{ox})(\text{H}_2\text{O})_2(\text{phen})]^+$ are the same.

There are several interesting features of the oxidations themselves that should be pointed out.

(a) There is an unexpectedly large difference in the reactivities of $[\text{Cr}(\text{ox})_2(\text{bpy})]^-$ and $[\text{Cr}(\text{ox})_2(\text{phen})]^-$ with permanganate. The former is exceedingly stable toward oxidation. Higher temperatures and longer times are required, and the only chromium-containing product detected under these conditions is chromate (CrO_4^{2-}). On the other hand, the 1,10-phenanthroline compound is rapidly oxidized to the dihydrate. This difference in reactivity may be due to steric effects (coordinated 2,2'-bipyridyl can twist);⁸ however, molecular models fail to show any steric differences likely to significantly affect permanganate attack.

(b) The absence of any detectable monotartrate-bridged species in the tartrate complex oxidations is unexpected and indicates either that both diols are cleaved simultaneously or that a monobridged complex is significantly more susceptible to further oxidation.

(c) It is interesting that the *meso*-tartrate and *d*-tartrate complexes, despite their large differences in geometry,³ react so similarly with permanganate. Of particular importance is the steric impossibility (shown by molecular models) for the *d*-tartrate complexes to form the cyclic manganese(VII) ester (2) given as a possible (though not necessarily likely) inter-



mediate in glycol-permanganate reactions.⁹ However, owing to the close approach of hydroxy oxygen atoms of different ligands in both the *meso*-tartrate and *d*-tartrate complexes,^{3,10} simultaneous coordination of oxygen atoms on different bridging ligands by permanganate is possible. Formation of such an intermediate could allow simultaneous (or nearly so) bridge cleavage.

Registry No. $\text{H}_2\text{Cr}_2(d\text{-tart})(\text{bpy})_2$, 57172-74-4; $\text{H}_2\text{Cr}_2(ms\text{-tart})(\text{bpy})_2$, 57172-56-2; $\text{H}_2\text{Cr}_2(d\text{-tart})(\text{phen})_2$, 57129-82-5; $\text{H}_2\text{Cr}_2(ms\text{-tart})(\text{phen})_2$, 57172-57-3; $[\text{Cr}(\text{H}_2\text{O})_2(\text{ox})(\text{phen})]\text{ClO}_4$, 77257-28-4; $\text{Cr}(\text{H}_2\text{O})(\text{OH})(\text{ox})(\text{phen})$, 77270-02-1; $\text{Na}[\text{Cr}(\text{ox})_2(\text{bpy})]$, 77257-29-5; $\text{K}[\text{Cr}(\text{ox})_2(\text{phen})]$, 14516-02-0; $\text{Na}[\text{HCr}_2(d\text{-tart})_2(\text{bpy})_2]$, 57129-83-6; $\text{Na}[\text{HCr}_2(d\text{-tart})_2(\text{phen})_2]$, 57129-85-8; $(\text{CD}^+)_{589}\text{-Na}[\text{HCr}_2(ms\text{-tart})_2(\text{bpy})_2]$, 57129-84-7; $(\text{CD}^-)_{537}\text{-}[\text{Cr}(\text{ox})(\text{H}_2\text{O})_2(\text{phen})]^+$, 77287-03-7.

- (9) Stewart, R. *Org. Chem. (N. Y.)* **1965**, 5, Chapter I.
 (10) An X-ray structure determination on $(\pm)\text{-Na}[\text{HCr}_2(ms\text{-tart})_2(\text{bpy})_2]\cdot 7\text{H}_2\text{O}$ shows a distance of 2.418 Å between hydroxyl oxygen atoms on separate bridges: Ortega, R. B. Ph.D. Dissertation, University of New Mexico, 1980.

Contribution from The Guelph-Waterloo Centre for Graduate Work in Chemistry, Department of Chemistry, Guelph Campus, University of Guelph, Guelph, Ontario, Canada N1G 2W1, the Department of Chemistry, University of New Brunswick, Fredericton, New Brunswick, Canada E3B 5A3, and the Department of Chemistry, Stanford University, Stanford, California 94305

Heteronuclear Mixed-Valence Ions Containing Ruthenium and Ferrocene Centers

Norman Dowling, Patrick M. Henry,* Nita A. Lewis,* and Henry Taube*

Received November 5, 1980

The study of binuclear mixed-valence complexes has accelerated steadily since the first such diruthenium species was reported by Creutz and Taube in 1969.¹ Various metal centers have now been reported to form symmetrical homonuclear weakly coupled structures, of which the most common examples are those containing two ruthenium or two ferrocene nuclei.²⁻⁴ Meyer and co-workers have also looked at the mixed-valence properties of unsymmetrical homonuclear diruthenium species of the type $[(\text{NH}_3)_3\text{RuLRuCl}(\text{bpy})_2]^{4+}$ ($\text{L} = \text{pyz}$, 4,4'-bpy, BPE).⁵ These unsymmetrical mixed-valence ions exhibited near-infrared intervalence-transfer (IT) bands

- (6) Kaizaki, S.; Hidaka, J.; Shimura, Y. *Bull. Chem. Soc. Jpn.* **1969**, 42, 988.
 (7) Broomhead, J. A.; Kane-Maguire, N.; Lauder, I. *Inorg. Chem.* **1970**, 9, 1243.
 (8) McKenzie, E. D. *Coord. Chem. Rev.* **1971**, 6, 187.

* To whom correspondence should be addressed: P.M.H., University of Guelph; N.A.L., University of New Brunswick; H.T., Stanford University.

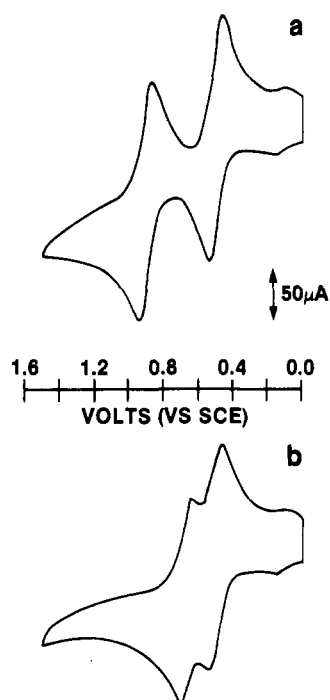


Figure 1. Cyclic voltammograms of (a) $[(\text{NH}_3)_5\text{RuNCFc}](\text{PF}_6)_2$ and (b) $[(\text{NH}_3)_5\text{RuNCCH}=\text{CHFc}](\text{PF}_6)_2$ in 0.1 M $[\text{N}(\text{C}_2\text{H}_5)_4]\text{ClO}_4\text{-CH}_3\text{CN}$ vs. SCE. The scan rate is 200 mV/s.

whose properties were in good agreement with the treatment provided by Hush,⁶ indicating weak electronic interaction between the metal centers.

As yet no heteronuclear mixed-valence complexes, in which there is some degree of valence delocalization between the metal centers, have been reported. Although $(\text{NH}_3)_5\text{Ru}^{\text{III}}\text{L-Fe}^{\text{II}}(\text{CN})_5$ ($\text{L} = \text{pyz}$) was originally believed to be partially delocalized,⁷ a more recent study has indicated the complexes ($\text{L} = \text{pyz}$, 4,4'-bpy) to be best described in terms of valence-trapped structures.⁸ This raises the interesting comparison between the fully valence-trapped heteronuclear ruthenium-iron complexes and the partially valence-delocalized structures of the dimeric ruthenium¹⁵ and iron⁹ species derived from each half of the heteronuclear ions.

In view of the known mixed-valence properties of suitably bridged dimeric ruthenium complexes as well as coupled ferrocene centers, it appeared that the potential interaction of these two types of nuclei via a suitable electron conducting bridge might afford the first heteronuclear mixed-valence species. Since the nitrile-containing molecules cyanogen¹⁰ and *tert*-butylmalononitrile¹¹ were found to be extremely good bridging groups in mixed-valence dimeric ruthenium complexes, the cyano moiety was tested as a bridging ligand in binuclear complexes containing ferrocene and ruthenium nuclei.

Table I. Redox Potentials of Ruthenium Complexes and Ferrocene Ligands^{a,b}

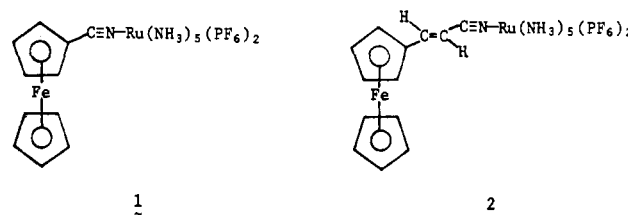
| | $E_{1/2}(\text{Ru}^{\text{III}}/\text{II}),$ V (ΔE_p , mV) | $E_{1/2}(\text{Fc}^{+/0}),$ V (ΔE_p , mV) |
|---|--|---|
| $[(\text{NH}_3)_5\text{RuNCFc}]^{2+}$ (1) | +0.44 (70) | +0.85 (80) |
| $[(\text{NH}_3)_5\text{RuNCFc}]^{2+}$ | +0.50 (70) | |
| FcCN | | +0.77 (100) |
| $[(\text{NH}_3)_5\text{RuNCCH}=\text{CHFc}]^{2+}$ (2) | +0.44 (74) | +0.66 (65) |
| $[(\text{NH}_3)_5\text{RuNCCH}=\text{CH}_2]^{2+}$ | +0.50 (60) | |
| FcCH=CHCN | | +0.56 (84) |

^a Pt working electrode in 0.1 M TEAP-acetonitrile vs. SCE.

^b Fc represents the ferrocenyl moiety.

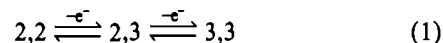
Results and Discussion

The heteronuclear complexes **1** and **2** were generated by



reaction of the aquo(pentaammine)ruthenium(II) ion with cyanoferrocene¹² and *trans*-acrylonitrileferrocene,¹³ respectively, in deaerated acetone. The isolated yellow-orange hexafluorophosphate salts gave the expected microanalyses and were further characterized by ¹H NMR (acetone-*d*₆) and infrared spectral analysis. The expected shift to lower wavenumber for the nitrile stretching band on going from free to coordinated ligand found for other ruthenium(II)-nitrile species was observed.¹⁴

Cyclic voltammograms of the fully reduced complexes **1** and **2** (Figure 1) exhibited two reversible waves in 0.1 M TEAP-acetonitrile in the potential range 0.0–1.5 V vs. the saturated calomel electrode, due to stepwise oxidation of the complex in two discrete one-electron steps (eq 1). The assignment of



these waves to the oxidation-reduction of a particular metal center was accomplished by comparison with the redox potential of a chosen model system. The complexes $[(\text{NH}_3)_5\text{RuNCFc}]^{2+}$ and $[(\text{NH}_3)_5\text{RuNCCH}=\text{CH}_2]^{2+}$ were selected as appropriate electrochemical models for the ruthenium(II) centers in the complexes **1** and **2**, respectively. As well the free ferrocene ligands were considered reasonable models for the coordinated molecules. The $E_{1/2}$ values for the binuclear ferrocene-ruthenium species as well as the model ruthenium complexes and ferrocene ligands are reported in Table I.

Comparison of the potential for the initial oxidation wave of +0.44 V for both **1** and **2** with the $E_{1/2}$ value of +0.50 V for the ruthenium(II) centers in the model complexes allows the assignment of this wave to the Ru(III)/Ru(II) couple in the binuclear species. The redox potentials of +0.77 V for cyanoferrocene and +0.56 V for *trans*-acrylonitrileferrocene further corroborate the above assignments. From Table I it can be seen that the potential for oxidation of the second center in the mixed-valence binuclear ions occurs 80–100 mV more anodic than that of the free ferrocene ligands. The shift to a more anodic potential is expected to arise as a result of the charge effect arising from the proximity of the ruthenium(III)

- Creutz, C.; Taube, H. *J. Am. Chem. Soc.* **1969**, *91*, 3988; **1973**, *95*, 1086.
- Cowan, D. O.; LeVanda, C.; Park, J.; Kaufman, F. *Acc. Chem. Res.* **1973**, *6*, 1.
- Tom, G. M.; Creutz, C.; Taube, H. *J. Am. Chem. Soc.* **1974**, *96*, 7827.
- LeVanda, C.; Bechgaard, K.; Cowan, D. O. *J. Org. Chem.* **1976**, *41*, 2700.
- (a) Callahan, R. W.; Brown, G. M.; Meyer, T. *J. Inorg. Chem.* **1975**, *14*, 1443. (b) Key: pyz = pyrazine; 4,4'-bpy = 4,4'-bipyridine; BPE = *trans*-1,2-bis(4-pyridyl)ethylene.
- Hush, N. S. *Prog. Inorg. Chem.* **1967**, *8*, 391.
- Toma, H. E.; Santos, P. S. *Can. J. Chem.* **1977**, *55*, 3549.
- Yeh, A.; Haim, A.; Tanner, M.; Ludi, A. *Inorg. Chim. Acta* **1979**, *33*, 51.
- Felix, F.; Ludi, A. *Inorg. Chem.* **1978**, *17*, 1782.
- Tom, G. M.; Taube, H. *J. Am. Chem. Soc.* **1975**, *97*, 5310.
- Krentzien, H.; Taube, H. *J. Am. Chem. Soc.* **1976**, *98*, 6379.

- Broadhead, G. D.; Osgerby, J. M.; Pauson, P. L. *J. Chem. Soc.* **1958**, 650.
- Kasahara, A.; Izumi, T.; Saito, G.; Yodono, M.; Saito, R. Goto, Y. *Bull. Chem. Soc. Jpn.* **1972**, *45*, 895.
- Clarke, R. E.; Ford, P. C. *Inorg. Chem.* **1970**, *9*, 227.

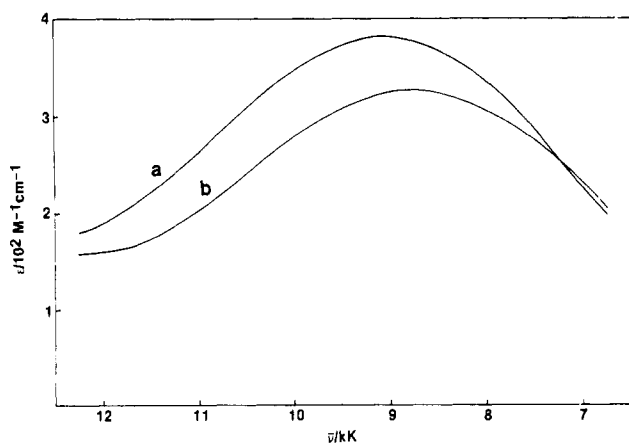


Figure 2. Near-infrared intervalence-transfer bands for 1.1×10^{-3} M solutions of (a) $[(\text{NH}_3)_5\text{Ru}^{\text{III}}\text{NCFc}]^{3+}$ and (b) $[(\text{NH}_3)_5\text{Ru}^{\text{III}}\text{NCCH}=\text{CHFc}]^{3+}$ in 0.1 M $[\text{N}(\text{C}_2\text{H}_5)_4]\text{ClO}_4\text{-CH}_3\text{CN}$.

center in the molecule as well as stabilization of the mixed-valence ion by electron delocalization over the metal centers. Hence the low-energy oxidation state isomers of the mixed-valence ions derived from **1** and **2**, respectively, have the structures $[(\text{NH}_3)_5\text{Ru}^{\text{III}}\text{NCFc}]^{3+}$ (**3**) and $[(\text{NH}_3)_5\text{Ru}^{\text{III}}\text{NCCH}=\text{CHFc}]^{3+}$ (**4**) containing oxidized ruthenium(III) centers.

The mixed-valence (2,3) ions were electrochemically generated by controlled-potential electrolysis at a Pt gauze electrode in both 0.1 M TEAP-acetonitrile and 0.12 M DCI- D_2O .¹⁵ The near-infrared spectra (Figure 2) of the mixed-valence ions **3** and **4** exhibited broad low-intensity bands at 1100 (ϵ 380) and 1143 nm (ϵ 330), respectively, in acetonitrile, which were absent from the spectra of the fully reduced and fully oxidized species.

In his theoretical treatment of intervalence-transfer transitions Hush derived eq 2 relating the energy of the IT trans-

$$\bar{\nu}_{\text{op}} - \bar{\nu}_0 = (\Delta\bar{\nu}_{1/2})^2 / 2.31 \quad (2)$$

sition $\bar{\nu}_{\text{op}}$ and the band half-width $\Delta\bar{\nu}_{1/2}$. $\bar{\nu}_0$ is the internal energy difference between the two oxidation state isomers. The value of $\bar{\nu}_0$, while not directly accessible from the electrochemical data, can be estimated to an upper limit by the difference in the redox potentials of the two centers in the molecule.¹⁷ For the mixed-valence nitrile-bridged ion, **3**, the above difference in potentials from Table I is 0.41 V ($\bar{\nu}_0 = 3.2 \times 10^3 \text{ cm}^{-1}$). With use of eq 2 a lower limit of $3.7 \times 10^3 \text{ cm}^{-1}$ is calculated for $\Delta\bar{\nu}_{1/2}(\text{calcd})$ the band half-width, compared to the corresponding observed value $\Delta\bar{\nu}_{1/2}(\text{obsd})$ of 4.9×10^3

cm^{-1} . The observed band half-width is therefore approximately 1.3 times the calculated value; a comparable result was obtained for the *trans*-acrylonitrile-bridged ion **4**. A similar order of agreement has also been found between observed and calculated values for several other symmetrical^{13,18} and unsymmetrical⁵ mixed-valence ions of the class II or weakly interacting type.

The solvent dependency of the near-infrared bands in the mixed-valence complexes further showed the expected behavior. In 0.12 M DCI- D_2O the absorption maxima for complexes **3** and **4** were found at 1036 and 1100 nm, respectively, a shift to shorter wavelength in agreement with the theoretical prediction made by Hush. On the basis of the above evidence the near-infrared bands have been assigned to intervalence-transfer transitions involving light-induced electron transfer between the metal centers. The appearance of these IT bands in the near-infrared spectra of the mixed-valence complexes further confirm the presence of weak metal-metal interaction between the dissimilar metal centers.

Hush further derived an expression for the interaction parameter α^2 (eq 3) which gives an approximate measure of the

$$\alpha^2 = \frac{(4.2 \times 10^{-4}) \epsilon_{\text{max}} \Delta\bar{\nu}_{1/2}}{\bar{\nu}_{\text{op}} d^2} \quad (3)$$

degree of ground-state delocalization in a mixed-valence complex, where ϵ_{max} is the molar extinction coefficient and d is the distance separating the metal centers. Using reasonable estimates of the internuclear separation, values for α^2 of 2.3×10^{-3} and 1.2×10^{-3} were calculated for the ions **3** and **4**, respectively. These values correspond closely with other reported values of α^2 for several class II mixed-valence ions.^{18,19}

These results indicate that weakly coupled heteronuclear mixed-valence ions can be prepared. Since ferrocene can be functionalized once or more on either of the two cyclopentadienyl rings the preparation of multinuclear systems becomes feasible and work is under way to prepare such ions based on the ferrocene moiety.²⁰

Experimental Section

Materials. Tetraethylammonium perchlorate (Eastman Organics) was recrystallized from hot water and dried under vacuum at 70 °C for 24 h. Acetonitrile (Eastman Organics, nonaqueous electrochemical solvent grade) was further dried by passing down an activated alumina (neutral, B.A. 1) column. DCI (35% w/w), D_2O (MSD Isotopes), and all other solvents were used without further purification. The ligands cyanoferrrocene¹² and *trans*-acrylonitrileferrocene¹³ were prepared by literature procedures. Argon was scrubbed by either passing it through an Oxisorb (Airco Industrial Gases) canister or through a chromous bubbler.

Preparations. $[(\text{NH}_3)_5\text{RuCl}]\text{Cl}_2$. This complex was prepared by the method of Vogt et al.²¹ and recrystallized from warm (40 °C) 0.1 M HCl.

$[(\text{NH}_3)_5\text{Ru}(\text{H}_2\text{O})](\text{PF}_6)_2$. The procedure outlined by Kuehn and Taube²² was used for the synthesis of this complex.

$[(\text{NH}_3)_5\text{RuL}](\text{PF}_6)_2$ ($\text{L} = \text{FcCN}$ and $\text{FcCH}=\text{CHCN}$). In a typical preparation $[(\text{NH}_3)_5\text{Ru}(\text{H}_2\text{O})](\text{PF}_6)_2$ (0.200 g, 0.41 mmol) was added to an argon deaerated solution of cyanoferrrocene (0.171 g, 0.81 mmol) in acetone (5 mL). The solution was allowed to react for ~2 h during which time it was agitated by bubbling a slow stream of argon through the solution. Addition of deaerated ether to the acetone solution precipitated the product (0.195 g, 70%) as an orange solid which was filtered in an argon atmosphere, washed with ether, and suction dried. Anal. Calcd for $[(\text{NH}_3)_5\text{RuNCC}_5\text{H}_4\text{FeC}_5\text{H}_5](\text{PF}_6)_2$: C, 19.24; H, 3.52; N, 12.24. Found: C, 19.05; H, 3.61; N, 12.66. Calcd for $[(\text{NH}_3)_5\text{RuNCCH}=\text{CHC}_5\text{H}_4\text{FeC}_5\text{H}_5](\text{PF}_6)_2 \cdot 2\text{H}_2\text{O}$: C, 21.34; H, 3.83;

(15) In contrast to the electrochemical results in acetonitrile the cyclic voltammogram in aqueous DCI- D_2O solution exhibited a reversible wave for the Ru(III)/Ru(II) couple but a chemically irreversible wave for oxidation of the ferrocenyl moiety. The chemical irreversibility of the ferrocenyl oxidation is attributed to the hydrolytic instability of the nitrile function¹⁶ on the fully oxidized (3,3) ion.

(16) Diamond, S. E.; Taube, H. *J. Chem. Soc., Chem. Commun.* **1974**, 622.

(17) For the nitrile-bridged ion **3**, $\bar{\nu}_0$ represents the internal energy change for the reaction $[(\text{NH}_3)_5\text{Ru}^{\text{III}}\text{NCFc}]^{3+} \rightarrow [(\text{NH}_3)_5\text{Ru}^{\text{II}}\text{NCFc}^+]$. Neglecting entropy changes ($\Delta S \approx 0$) gives the approximate relation $\bar{\nu}_0 \approx \Delta G$. The free energy difference between the two oxidation state isomers, ΔG , can be calculated from the difference in the redox potentials of the two couples $[(\text{NH}_3)_5\text{Ru}^{\text{III}}\text{NCFc}^+]/[(\text{NH}_3)_5\text{Ru}^{\text{II}}\text{NCFc}^{2+}]$ (E_1), and $[(\text{NH}_3)_5\text{Ru}^{\text{III}}\text{NCFc}^{3+}]/[(\text{NH}_3)_5\text{Ru}^{\text{II}}\text{NCFc}^{2+}]$ ($E_2 = 0.44$ V, Table I). The E_1 couple however is experimentally unobservable. A reasonable estimate of this value is provided by the related redox couple $[(\text{NH}_3)_5\text{Ru}^{\text{III}}\text{NCFc}^+]/[(\text{NH}_3)_5\text{Ru}^{\text{II}}\text{NCFc}^{2+}]$ (0.85 V, Table I), which gives $\Delta G \approx \bar{\nu}_0 \approx 0.41$ V ($3.2 \times 10^3 \text{ cm}^{-1}$). The couple $[(\text{NH}_3)_5\text{Ru}^{\text{III}}\text{NCFc}^+]/[(\text{NH}_3)_5\text{Ru}^{\text{II}}\text{NCFc}^{2+}]$ can be seen to represent an upper-limit to the value of E_1 , as both stabilization of the mixed-valence (2,3) ion as well as a slightly greater electrostatic effect will cause the above couple to occur at a more anodic potential relative to the E_1 couple.

(18) Callahan, R. W.; Keene, F. R.; Meyer, T. J.; Salmon, D. J. *J. Am. Chem. Soc.* **1977**, *99*, 1064.

(19) Powers, M. J.; Meyer, T. J. *J. Am. Chem. Soc.* **1978**, *100*, 4393.

(20) Dowling, N., unpublished results.

(21) Vogt, L. H., Jr.; Katz, J. L.; Wiberley, S. E. *Inorg. Chem.* **1965**, *4*, 1157.

(22) Kuehn, C. G.; Taube, H. *J. Am. Chem. Soc.* **1976**, *98*, 689.

N, 11.49. Found: C, 21.47; H, 4.01; N, 11.18.

Electrochemistry. Cyclic voltammetry was performed with a PAR Model 170 Electrochemistry System in a conventional three compartment electrochemical cell. Formal potentials were determined at a Pt flag working electrode relative to the saturated calomel electrode (SCE) at $22 \pm 2^\circ\text{C}$. Measurements were carried out on millimolar concentrations of the complexes in acetonitrile solution containing 0.1 M $[(\text{C}_2\text{H}_5)_4\text{N}]\text{ClO}_4$ (TEAP) supporting electrolyte as well as in 0.12 M DCl-D₂O solution.

$E_{1/2}$ values for the Ru(III)/Ru(II) couples were taken as the average of the anodic and cathodic peak potentials. Electrochemical reversibility was based on the peak-to-peak separation (ΔE_p) for the complementary anodic and cathodic cyclic voltammetric waves relative to the theoretically predicted value of 59 mV for a one-electron redox process.

Near-Infrared Spectra. Near-infrared spectra were run on 1.1×10^{-3} M solutions on a Cary Model 14 spectrophotometer over the wavelength range 1600–800 nm. Solutions of the half-oxidized mixed-valence ions were generated by controlled potential electrolyses in the same three compartment electrochemical cell using a semi-

cylindrical Pt gauze electrode. A solution of known concentration of the fully reduced (2,2) ion was prepared in the argon-deaerated electrochemical solvent of choice and loaded into an argon-flushed electrochemical cell by syringe technique, taking care to avoid dilution from solvent in the auxiliary electrode compartment. After exhaustive electrolysis the solution was transferred by syringe technique to an argon-flushed 1-cm quartz cell fitted with a special Teflon inert valve.

Acknowledgment. P.M.H. and N.A.L. thank the Natural Science and Engineering Research Council of Canada for a coop grant in support of this research. We both also wish to thank H.T. for his hospitality while we were at Stanford University. P.M.H. was on sabbatical leave during the winter and spring of 1978, and N.A.L. was a NRC postdoctoral fellow 1977–1979. This work was initiated during that period.

Registry No. 1, 77482-12-3; 2, 77482-14-5; 3, 77482-15-6; 4, 77482-16-7; $[(\text{NH}_3)_5\text{RuNCPH}]^{2+}$, 31418-68-5; $[(\text{NH}_3)_5\text{RuNCCH}=\text{CH}_2]^{2+}$, 44916-13-4; $[(\text{NH}_3)_5\text{Ru}(\text{H}_2\text{O})](\text{PF}_6)_2$, 34843-18-0; FcCN , 1273-84-3; $\text{FcCH}=\text{CHCN}$, 32626-63-4.

Correspondence

Application of the Vibronic Coupling Model to a Series of Binuclear Mixed-Valence Ruthenium Complexes

Sir:

Mixed-valence properties of binuclear complexes $\text{X}_3\text{M}^{\text{II}}\text{LM}^{\text{III}}\text{X}_3$ have been recently discussed by Schatz and co-workers¹ in terms of a vibronic coupling model. The essential step of this approach consists in the computation of the absorption band profile of the low-energy intervalence transition (IT), emphasizing its vibronic nature. The crucial vibrational coordinate q is represented by the antisymmetric combination of the normal coordinates for the breathing mode of the two constituent subunits $\text{M}^{\text{II}}\text{X}_6$ and $\text{M}^{\text{III}}\text{X}_6$, assumed to be adequately described by octahedral symmetry. Two parameters of this one-dimensional problem essentially define the mixed-valence behavior, the vibronic coupling λ and the electronic coupling ϵ . The vibronic coupling is shown to be proportional to Δr , the difference of the metal–ligand distances in the M(II) and M(III) subunits.^{1b} The potential energy surfaces related to the intervalence transfer are given by eq 1, where W , as well as ϵ and λ , is expressed in units of ν , the

$$W_{1,2} = \frac{q^2}{2} \pm (\epsilon^2 + \lambda^2 q^2)^{1/2} \quad (1)$$

wavenumber of the totally symmetric stretching vibration of the mononuclear subunits. In order to facilitate calculations the approximation $\nu(\text{M}^{\text{II}}\text{X}_6) = \nu(\text{M}^{\text{III}}\text{X}_6)$ is made.

ϵ , λ , and ν define the complete vibronic manifold, and hence the shape of the IT band can be calculated as the superposition of transitions between vibronic levels. Two limiting situations are obtained from eq 1: (i) for $\epsilon \approx 0$ (localized limit), $W_2 - W_1 \approx 2\lambda q$; (ii) for $\lambda \approx 0$ (delocalized limit), $W_2 - W_1 \approx 2\epsilon$. The condition $dW_1/dq = 0$ for eq 1 defines potential minima at $q_{\text{min}} = \pm((\lambda^4 - \epsilon^2)/\lambda^2)^{1/2}$. Thus, crossover from the valence-trapped (two minima, class II according to Robin and Day²) to the valence-delocalized case (one minimum at $q = 0$, class III) occurs when $|\epsilon|$ approaches λ^2 . With the observed

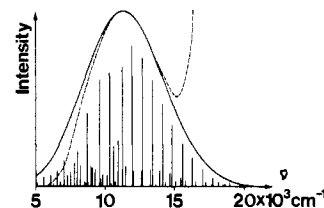
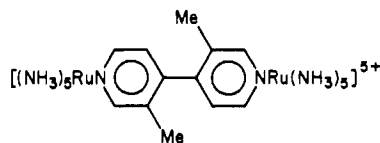


Figure 1. Observed (broken line)⁸ and calculated (solid line) intervalence band for



The vertical sticks represent individual vibronic transitions, their intensities scaled by the Boltzmann population factor. The best fit corresponds to $\epsilon = -2.46$ and $\lambda = 3.58$.

energy $W_2 - W_1$ of the IT band and the appropriate limit, reasonable starting values for ϵ and λ are estimated for computing band shapes. The best fit of the calculated band to the experimental one is obtained by a systematic variation of λ and ϵ .

The application of the vibronic coupling model to the pyrazine-bridged ruthenium dimer, the Creutz-Taube complex, led to the conclusion that this mixed-valence species is strongly delocalized.^{1b} In order to test the range of validity of the model, we calculated IT band shapes for a series of mixed-valence ruthenium complexes, the mononuclear species being either $\text{Ru}(\text{NH}_3)_5$ or $\text{Ru}(\text{bpy})_2\text{Cl}$. Whenever possible we used the line drawings of published solution spectra; otherwise the comparison between observed and calculated spectra was based on the energy, the intensity, and the half-width of IT bands reported in the literature. The resulting model parameters ϵ and λ as well as the spectroscopic data (1–16 measured in D₂O, 17 and 18 in acetonitrile) are summarized in Table I. A representative example is illustrated in Figure 1. The solvent dependence of IT band positions for localized complexes implies a solvent dependence of λ . Medium effects on band intensity and half-width, however, are not reported. This phenomenon therefore could not be considered in our analysis. The close proximity of the solvent parameters for D₂O and

(1) (a) Piepho, S. B.; Krausz, E. R.; Schatz, P. N. *J. Am. Chem. Soc.* 1978, 100, 2996. (b) Schatz, P. N.; Wong, K. Y. *Prog. Inorg. Chem.*, in press.
(2) Robin, M. B.; Day, P. *Adv. Inorg. Chem. Radiochem.* 1967, 10, 247.